

## On the recent observation of the hadroproduction of prompt photons

F. Halzen and D. M. Scott

*Physics Department, University of Wisconsin—Madison, Madison, Wisconsin 53706*

(Received 13 November 1979)

The recent observations of prompt photons in hadron collisions are confronted with the predictions of perturbative quantum chromodynamics, with very encouraging results. We discuss the data, and comment on their experimental and theoretical implications.

### I. INTRODUCTION AND REVIEW

The observation of high-transverse-momentum ( $p_T$ ) prompt photons in high-energy  $p$ Be (Ref. 1) and  $pp$  (Ref. 2) collisions has recently been reported. The existence of prompt photons populating the high- $p_T$  region is required by quantum chromodynamics (QCD): the photon couples to the electric charge of quarks in a pointlike manner; therefore the fast quarks responsible for the abundant production of hadrons with large  $p_T$  will radiate and be the origin of prompt photons in the same kinematic range. The prompt-photon cross sections have been calculated in perturbative QCD,<sup>3-8</sup> and the measured cross sections are of the predicted order of magnitude. Here we wish to make a detailed comparison between data and theoretical calculations.

In lowest-order QCD the diagrams responsible for the production of high-transverse-momentum real photons are those shown in Figs. 1(a) and 1(b). The cross sections for these parton subprocesses are given, respectively, by

$$\frac{d\sigma^{gq}}{dt} = \frac{\pi\alpha\alpha_s}{3} \frac{s^2+u^2}{s^3(-u)}, \quad (1a)$$

$$\frac{d\sigma^{q\bar{q}}}{dt} = \frac{\pi\alpha\alpha_s}{9} \frac{t^2+u^2}{s^2tu}. \quad (1b)$$

Here  $g$  ( $q$ ) stands for gluon (quark),  $s$ ,  $t$ ,  $u$  are the usual Mandelstam invariants for the subprocess, and  $\alpha_s = 1.51/\ln(p_T^2/0.25 \text{ GeV}^2)$  is the strong fine-structure constant. The convolution over initial parton densities giving the cross section  $E d\sigma/d^3p$  to be compared to data is described in detail in Ref. 3, including a particular choice of parton densities.

The data<sup>1,2</sup> for  $\gamma/\pi^0$  are shown in Fig. 2, plotted as a function of  $p_T$  for various energies. The calculated  $\gamma/\pi^0$  ratio is shown for comparison. This quantity has been obtained from the QCD prompt-photon spectrum divided by a parametrization of the measured  $\pi^0$  cross section<sup>9-14</sup> [we take  $(\pi^+ + \pi^-)/2$  for  $p_T \geq 4 \text{ GeV}$ , for  $\sqrt{s} = 19.4$ ,

23.8 GeV (Ref. 15)]. We note that this simple QCD calculation predicted<sup>3</sup> prompt-photon cross sections in very good agreement with the CERN ISR data, and consistent with the highest- $p_T$  Fermilab data. Notice, however, that for  $p_T$  values in the range 1.5–3.5 GeV the calculation falls well below the Fermilab measurements. We note, however, that the calculations of  $\gamma/\pi^0$  are actually for production at  $90^\circ$ . The Fermilab experiment has a wide acceptance,  $160^\circ < \theta < 90^\circ$ , and finds some increase of  $\gamma/\pi^0$  with increasing  $x_F$ . This would indicate that  $\gamma/\pi^0$  at  $90^\circ$  for  $\sqrt{s} = 19.4$ , 23.8 GeV would be somewhat lower than shown in Fig. 2. The effect is less than a factor of 2. The statistical level of the data sample did not allow the detailed study of  $\gamma/\pi^0$  versus  $p_T$  in bands of  $x_F$  which would be needed in order to clearly separate the  $p_T$  and  $x_F$  behavior. Further discussion is given by Cox.<sup>1</sup>

A useful way to study the energy dependence of the data is to plot it in the form

$$\frac{\gamma}{\pi} = (p_T)^n f(x_T = 2p_T/\sqrt{s}), \quad (2)$$

with

$$n = n_\pi - n_\gamma.$$

Indeed, up to logarithms, QCD implies that both the  $\gamma$  and  $\pi$  cross sections exhibit the scaling of Eq. (2) with  $n_\pi = n_\gamma = 4$  and therefore  $n = 0$ . The logarithms and soft (small- $x_T$ ) effects modify  $n$  so that it is no longer a constant. We may still consider effective values, valid locally, and it is well known that  $n_\pi^{\text{eff}} \approx 8$  instead of 4 in order to recover agreement with the data. Because of the absence of a fragmentation function in the final state and its associated scaling violations we expect  $n_\gamma^{\text{eff}} < n_\pi^{\text{eff}}$ . In conclusion

$$0 < n^{\text{eff}} < 4.$$

Note that the constituent-interchange-model (CIM) calculation, which we will discuss further on, predicts  $n = 2$  ( $n_\gamma = 6$ ,  $n_\pi = 8$ ). The data indicates  $n = 1-2$ ; see Figs. 3(a), 3(b).

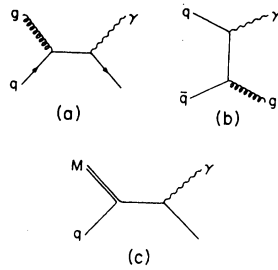


FIG. 1. Diagrams for the hadroproduction of high- $p_T$  photons: (a) QCD gluon-quark "Compton" scattering; (b) QCD quark-antiquark annihilation; (c) CIM meson-quark scattering.

## II. A CRITIQUE OF QCD COMPUTATIONS AND ALTERNATIVE SOURCES OF DIRECT PHOTONS

Our inability to accommodate the low- $p_T$ , low- $\sqrt{s}$  data raises the possibility of alternative sources of direct photons, such as the meson-quark scattering graph of Fig. 1(c). Alternatively it could just reflect our inability to do quantitative QCD calculations when venturing into the small- $p_T$  kinematic range. We first ask how unambiguous the QCD predictions are, and will subsequently address the question of alternative sources. The calculations shown in Fig. 2 are in the context of

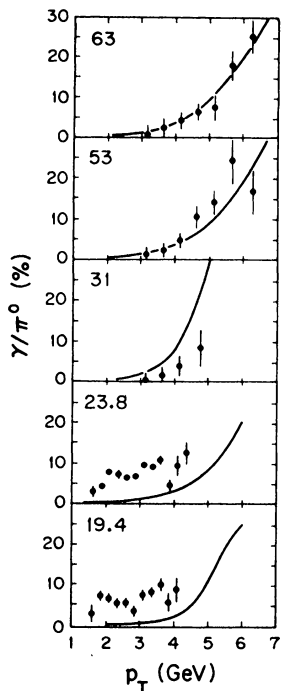


FIG. 2. The QCD calculation of  $\gamma/\pi^0$  of Ref. 3 is compared to data at various energies. The data at  $\sqrt{s} = 19.4$  and  $23.8$  GeV come from Ref. 1, and those at  $\sqrt{s} = 31, 53,$  and  $63$  GeV come from Ref. 2.

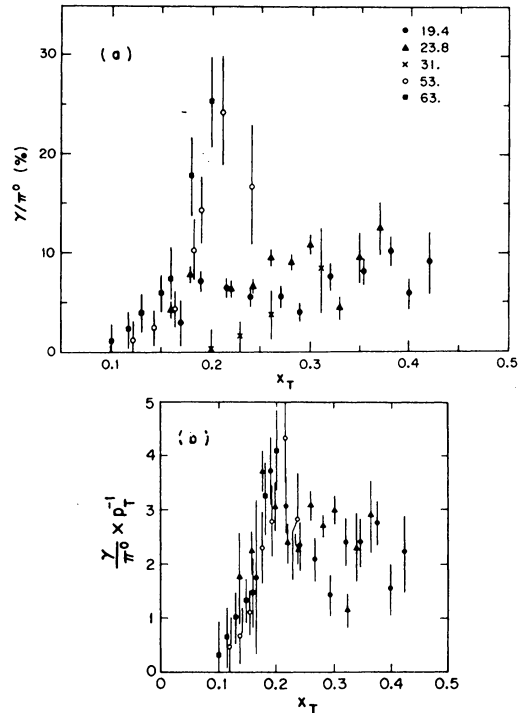


FIG. 3. (a) Data on  $\gamma/\pi^0$  plotted as a function of  $x_T = 2p_T/\sqrt{s}$ . (b) Data on  $\gamma/\pi^0$  (in percent) divided by  $p_T$  (in GeV) and plotted as a function of  $x_T$ .

a straightforward hard-scattering formalism, and no parton transverse momentum or logarithmic corrections have been considered. These are known to be important in order to quantitatively explain  $\pi^0$  production at intermediate  $p_T$  values in terms of lowest-order QCD graphs. The fact that we agree with the ISR prompt-photon data for  $p_T < 6$  GeV might then be surprising. However, we note that the calculation of prompt photons is cleaner than that of mesons, in that the photons are produced directly via a pointlike coupling, whereas the mesons are produced via parton fragmentation. We now systematically discuss various sources of uncertainty in the calculation.

(i) *Soft effects.* The QCD calculation diverges as  $p_T \rightarrow 0$  so that further regularization of the calculation could alter the results. This divergence also occurs in the closely related context of highly virtual photon (lepton pair) production with  $p_T \approx 0$ . (For a recent review and references, see Ref. 16. Calculation details are given in Ref. 3, and regularization details in Ref. 17.) Here the diagrams of Figs. 1(a) and 1(b) are again calculated, but with the outgoing photon off-shell. The real-photon calculation can therefore be directly normalized<sup>3</sup> using data on high-transverse-momentum lepton pairs. Indeed, the diagrams of Fig. 1(a), 1(b) are the source of both of them. The

resulting  $\gamma/\pi$  yield is shown as a dashed line in Fig. 4.

(ii) *Scaling violations.* Our parton densities are "effective" densities, which in principle should exhibit scaling violations, which are surely relevant. However, in practice, the uncertainty provided by scaling violations is complemented by uncertainty in the initial (at the renormalization point) shape of the gluon density. Because these two aspects of scaling violations tend to compensate, the net result of their inclusion can either enhance or decrease the  $\gamma/\pi$  ratio. Because our scaling parton densities are in agreement with data on lepton-pair  $p_T$  spectra and  $p_T$  integrated cross sections,<sup>18</sup> we believe they represent correct effective densities. The calculations using three different choices of parton densities are shown in Fig. 5, compared to the measured  $\pi^0$  cross section, at  $\sqrt{s}=53$  GeV and  $90^\circ$  in the center of mass. The solid curve is the prediction of Ref. 3; the dashed curve uses the scaling violating densities of Ref. 6; the dotted curve is a different implementation of scaling violations.<sup>5,19</sup> Note that at high  $p_T$  the two photons from the decay  $\pi^0 \rightarrow \gamma\gamma$  are not resolved, and consequently the measured cross section is actually for  $\pi^0$  plus prompt photon.

The level of uncertainty provided by (i) and (ii) above is further demonstrated in Fig. 4, where data at  $p_{\text{lab}}=200$  GeV is compared to four different calculational possibilities.

(iii) *Angular dependence.* The Fermilab data<sup>1</sup> is taken over a wide range of  $x_F$ , in the center-of-mass angular range  $90^\circ < \theta < 160^\circ$ . The ISR data is taken over an angular range about  $90^\circ$  in the center of mass. In order to measure  $\gamma/\pi^0$  it is important to know

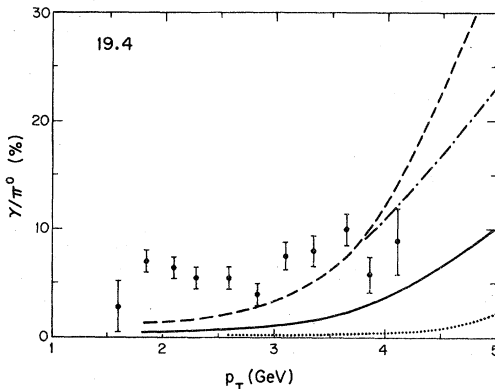


FIG. 4. Data (Ref. 1) on  $\gamma/\pi^0$  at  $\sqrt{s}=19.4$  GeV are compared with QCD calculations using the parton densities of Ref. 3 (solid line), Ref. 6 (dashed-dotted line), and Ref. 19 (dotted line). The dashed line is the QCD calculation normalized directly to the lepton pair data. The dramatic rise of the curves at  $p_T \approx 4$  GeV comes from the rapid falloff of the measured  $\pi$  cross sections.

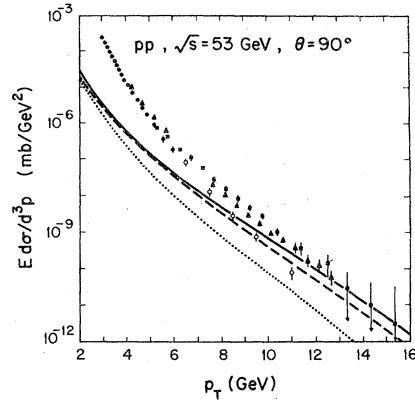


FIG. 5. QCD calculations of direct photons are compared to  $\pi^0$  data. The solid, dashed, and dotted lines use the parton densities of Refs. 3, 6, and 19, respectively. The data are from Refs. 20, 11, 12, and 21.

the angular dependence of the photon cross section. Our results for this are shown in Figs. 6(a) and 6(b), where the cross sections at  $\sqrt{s}=19.4$  and 53 GeV are plotted as a function of center-of-mass angle  $\theta_{\text{c.m.}}$  for various fixed  $p_T$  values. The Fermilab group also analyzed the  $x_F$  dependence of the data. The excess of observed photons for large values of  $x_F$  is difficult to accommodate using any type of hard-scattering mechanism. The excess may be connected to the fact that the fixed angular acceptance forces  $p_T$  to become large as  $x_F$  becomes large, and large  $p_T$  is where  $\gamma/\pi^0$  increases.

(iv) *Atomic-number dependence.* A further complication is that the Fermilab experiment is carried out on beryllium. If one writes the  $\pi$  cross section as varying as  $A^{\alpha_\pi(p_T)}$  with atomic number  $A$ , then for  $p_T \lesssim 6$  GeV  $\alpha_\pi(p_T)$  is an increasing function of  $p_T$ .<sup>15</sup> Presumably the same is true for the corresponding  $\alpha_\gamma(p_T)$ , but because of the electromagnetic, as opposed to strong, coupling of the photons to hadrons  $\alpha_\gamma(p_T) < \alpha_\pi(p_T)$ . Consequently,  $\gamma/\pi^0$  should be smaller in  $p\text{Be}$  collisions than in  $p\text{p}$  collisions. This makes a possible discrepancy between calculation and data for the lower- $p_T$  200-GeV data even greater.

The ambiguities in calculating  $\gamma$  spectra at intermediate  $p_T$  are further clouded by the possibility of additional sources, such as constituent-interchange-model (CIM) mechanisms.<sup>4,7,22</sup> In the CIM the dominant mechanism for producing high- $p_T$  prompt photons is  $q_1 M \rightarrow q_2 \gamma$ , where  $M$  is a meson; the diagram is shown in Fig. 1(c). The subprocess cross section is

$$\frac{d\sigma}{dt} = \frac{2\pi\alpha\alpha_M}{s^2} \frac{s^2+u^2}{(-t)} \left( \frac{e_{q_1}}{u} + \frac{e_{q_2}}{s} \right)^2, \quad (3)$$

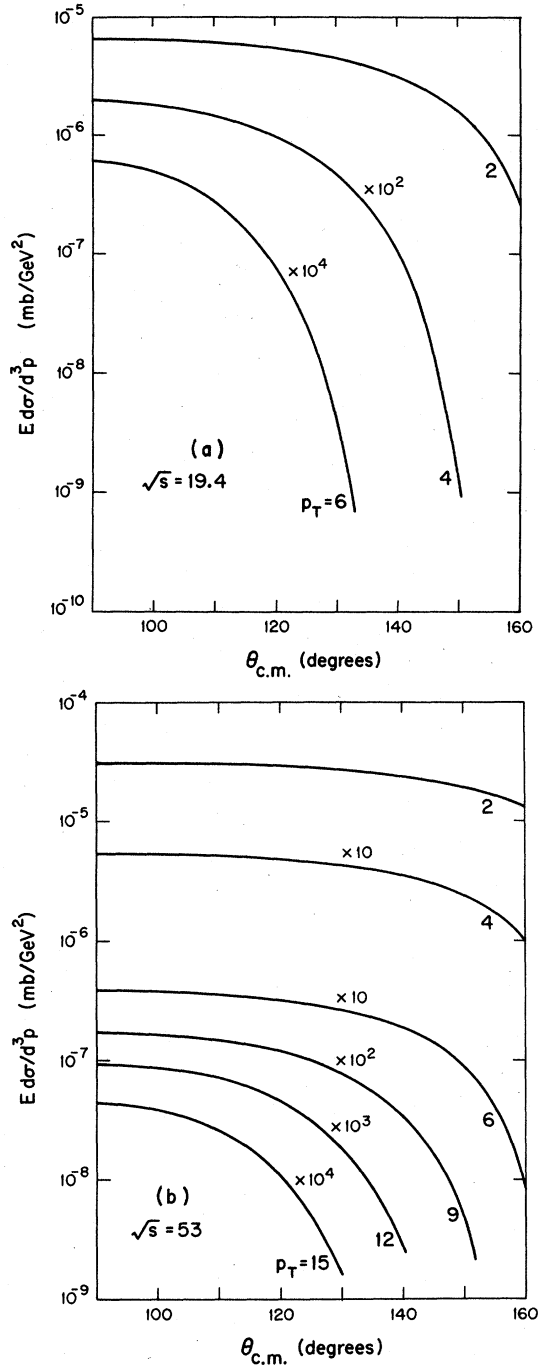


FIG. 6. Angular dependence of prompt-photon cross sections calculated in QCD. Some of the curves have been multiplied by powers of 10, as indicated.

where  $\alpha_M \approx 2$  GeV is the coupling of a meson to  $q\bar{q}$ , and  $e_{q_i}$  is the charge of quark  $q_i$ . The calculation, including quark and meson densities is described in detail in Ref. 4. Our results are in good agreement with the approximate methods

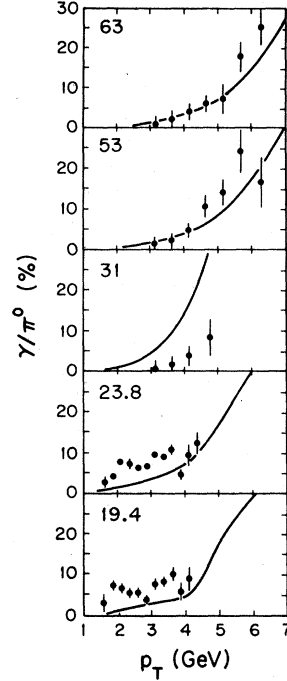


FIG. 7. The CIM calculation of  $\gamma/\pi^0$  is compared to data at various energies.

used in Ref. 4.

Again normalizing the calculated  $\gamma$  yield to the measured  $\pi$  spectrum, we show  $\gamma/\pi$  calculated in the CIM compared to the data in Fig. 7. We have two comments. First, the calculated curves are very similar, both qualitatively and quantitatively, with those calculated from QCD. Second, the CIM cannot explain the lower  $p_T$   $\gamma/\pi^0$  measured at Fermilab—if one increases the CIM result by a factor of 2, it would be inconsistent with the ISR result. Adding together the QCD and CIM results leads to similar conclusions. We note, however, that over the presently measured kinematic range, the CIM results are very similar to those from QCD.

Explicit consideration of parton transverse form factors and additional CIM-type contributions have been advocated to carry perturbative QCD calculations into the intermediate  $p_T$  range. To accommodate the  $\gamma/\pi$  data over the full energy range seems to challenge the quantitative aspects of both approaches.

### III. FURTHER EXPERIMENTAL AND THEORETICAL IMPLICATIONS

As we have already discussed, the measured high- $p_T$   $\pi^0$  cross section, where the two photons from the decay  $\pi^0 \rightarrow \gamma\gamma$  cannot be resolved, is actually the cross section for  $\pi^0$  plus prompt

photon. It may be possible to exploit this fact to make an experimental estimate of the direct photon yield in an experiment<sup>13</sup> where both charged and neutral pions are detected. If a high-transverse-momentum pion is produced from the fragmentation of a high-transverse-momentum quark or gluon, then using isospin symmetry we find for the high- $p_T$  yields,

$$\pi^0 = \frac{1}{2}(\pi^+ + \pi^-). \quad (4)$$

An excess of the  $\pi^0$  yield above this value, when known sources of photons such as  $\eta$  have been subtracted,<sup>13</sup> may be attributed to direct photons. Applying this procedure to the results of the CERN-Columbia-Rockefeller-Saclay experiment<sup>13</sup> gives  $\gamma/\pi \sim 20\%$  in the range  $3 \leq p_T \leq 6$  GeV, at  $\sqrt{s} = 63$  GeV, consistent with the measurements of Ref. 2.

Further information may be obtained through studying the jet on the away side from a high- $p_T$  direct photon. Indeed such measurements may help in their detection. The cross section for the production of a high- $p_T$  photon of momentum  $p$  and rapidity  $y$ , together with an away-side jet (parton) of rapidity  $y_J$  is

$$\frac{Ed\sigma}{d^3p dy_J} = \frac{1}{\pi} \frac{d\sigma^{\text{SP}}}{dt} x_1 f^B(x_1) x_2 f^T(x_2), \quad (5)$$

where

$$x_{1,2} = \frac{1}{2} x_T (e^{\pm y} + e^{\pm y_J}),$$

$$x_T = \frac{2p_T}{\sqrt{s}}, \quad (6)$$

and where  $f^B$  ( $f^T$ ) is the parton density in the beam (target).  $\sigma^{\text{SP}}$  is the subprocess cross section.

In  $pp$  collision, the dominant mechanism in QCD for producing high- $p_T$  direct photons is quark-gluon scattering.<sup>3</sup> So a measurement of the cross section in Eq. (5) would give a direct determination of the gluon density in the proton, as the quark density is already known from lepton-production experiments. Further, the away-side jet will dominantly be a quark, and then specializing to  $y = y_J = 0$  we have for the distribution of a hadron  $h$  in the away-side jet in terms of its fractional momentum  $z = p_T^h/p_T^J$ ,

$$\frac{dN^h}{dz} = \frac{\sum e_q^2 q(x_T) D_q^h(z)}{\sum e_q^2 q(x_T)}, \quad (7)$$

where  $e_q$  is the charge of quark  $q$ ,  $q(x)$  is its distribution in a proton, and  $D_q^h$  describes the fragmentation  $q \rightarrow h$ . Note that this is the same distribution as for hadrons produced in the parton fragmentation region in deep inelastic lepton scattering from a proton target. The resulting hadron distribution may be noticeable in that (i) the prod-

uction of positive particles is enhanced, and (ii) the spectrum is harder, compared to away-side hadrons produced opposite a high- $p_T$   $\pi^0$  trigger.

We comment that in  $p\bar{p}$  collisions, the dominant mechanism for high- $p_T$  direct photon production is  $q\bar{q} \rightarrow \gamma g$ . The away-side jet comes from gluon fragmentation.

The production of prompt photons at high  $p_T$  necessarily leads to the production of prompt leptons, which come in pairs.<sup>16,23</sup> The photons undergo internal conversion, producing an important source of prompt leptons. The lepton spectrum can be easily calculated<sup>23</sup> from the prompt-photon spectrum, using a bremsstrahlung approximation, and the result, at  $\sqrt{s} = 53$  GeV and  $90^\circ$  in the center of mass, is shown in Fig. 8, normalized to  $\pi$  data and compared to available data.<sup>24</sup> Note that the once mystical lepton-pion ratio  $l/\pi \approx 10^{-4}$  is now seen as a transient value for  $p_T$  values in the resonance region  $m_\rho/2 \leq p_T \leq m_\psi/2$ . Prompt photons produced from bremsstrahlung by (a) charged hadrons<sup>25</sup> for  $p_T \leq m_\rho/2$ ; (b) quarks for  $p_T \geq m_\psi/2$ , provide sources of direct leptons in excess of the  $l/\pi \approx 10^{-4}$  ratio. Because of the bremsstrahlung origin of the  $l/\pi$  ratio, we clearly expect that  $e/\pi > \mu/\pi$ , both at small ( $p_T \lesssim 1$ ) and large ( $p_T \gtrsim m_\psi/2$ ) transverse momentum. We need not list again the uncertainties involved in the calculation. We simply note that this mechanism, along with others calculable in QCD,<sup>26,27</sup> leads to copious prompt lepton production at high transverse momentum.

The increased  $\gamma/\pi$  and  $l/\pi$  ratio with decreasing transverse momentum due to the enhanced bremsstrahlung of charged secondaries draws our attention to the fact that the problem of prompt photons is potentially interesting, whatever the kinematic range of  $p_T$ . Although we escaped to the large- $p_T$  region to recover simple perturbative

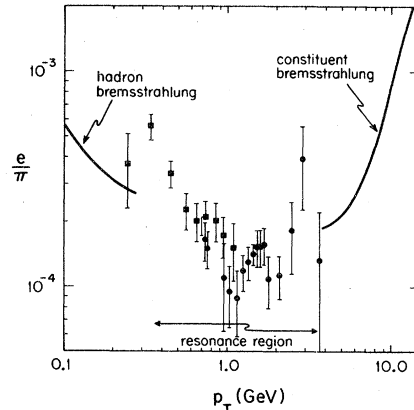


FIG. 8. Calculations of  $e/\pi$  are compared to data at  $\sqrt{s} = 53$  GeV,  $90^\circ$ .

QCD dynamics, the "gammaization" of hadron collisions was predicted<sup>28</sup> in 1962 by E. L. Feinberg, with no restriction on the transverse momentum of the secondaries. His proposal essentially consists in calculating the "background radiation" from a hadron collision. We reproduce it below, to illustrate its importance and the unusual and exciting possibilities that could be revealed in studies of  $\gamma/\pi$  ratios in the small- $p_T$  regime. Colliding hadrons swiftly pump their energy in a limited volume of hadronic matter. After expansion it reaches freeze-out and produces hadrons. Before cooling down, however, charge fluctuations result in the radiation of photons. If we model the charge fluctuations in terms of  $n_\pi$   $\pi$  mesons interacting (i.e., colliding or annihilating)  $\nu$  times, then ( $t$  is time here)

$$\frac{dn_\gamma}{dt} \cong n_\pi \nu \alpha. \quad (8)$$

This goes on for a characteristic time

$$t \cong V^{1/3} \cong (n_\pi/m_\pi^3)^{1/3}. \quad (9)$$

This is the time it takes to form physical hadrons (every  $\pi$  meson is assumed to occupy one Compton wavelength and therefore occupy a volume  $V \cong n_\pi/m_\pi^3$ ). From Eqs. (4), (5) we obtain

$$\frac{n_\gamma}{n_\pi} = C \alpha n_\pi^{1/3} \quad (10)$$

with  $C \approx 10$ . Therefore,  $n_\gamma/n_\pi \approx 15\%$  at  $\sqrt{s} = 50$  GeV where  $n_\pi \approx 12$ ; notice, however, that  $n_\gamma/n_\pi$  will exceed unity at energies in the  $10^2$ - $10^3$  TeV range (in this type of model  $n_\pi \propto \sqrt{s}$ ).

If indeed a large fraction of the produced hadrons, and not just the high-transverse-momentum secondaries, are photons at energies above typically 100 TeV, their signature should be dramatic even in the most routine cosmic-ray experiments above that energy. They have most likely been observed. In extensive-air-shower experiments one observes the production of charged and neutral  $\pi$  mesons in a cosmic-ray interaction via the development through the atmosphere of an electromagnetic shower with two components, a muon and an electron-photon component, originating respectively from charged- and neutral- $\pi$  decays. The energy deposited into the components is in the ratio

$$\frac{E_\gamma}{E_\mu} = \frac{\pi^0}{\pi^0 + \pi^+ + \pi^-} = \frac{1}{3}.$$

It is clear that if photons become a major part of the secondaries this ratio will increase and reach a value of

$$\frac{2\gamma + \pi^0}{2\gamma + \pi^0 + \pi^+ + \pi^-} = \frac{3}{5}$$

when  $\gamma/\pi = 1$ . Here we took into account the two polarization states of the  $\gamma$ . There is a wealth of literature corroborating this trend.<sup>29</sup> Anomalous development of the  $e-\gamma$  component of air showers has been observed. The anomaly appears around 10 TeV and becomes dramatic above 100 TeV. Anomalous development of air showers in calorimeter experiments has been interpreted as an increase in  $E_\gamma/E_\mu$  by about a factor of 2 as required by gammaization. Direct evidence for production of photons in isolated events above 100 TeV has recently been presented.

To conclude, the observation of prompt photons at the present levels is very encouraging for QCD. Their existence is predicted by QCD, and a detailed comparison of calculation and data at high  $p_T$  and energy can give important information about quark densities and scaling violations. In particular, the dominant  $O(\alpha_s)$  QCD subprocess for high- $p_T$  prompt-photon production in  $pp$  collisions is  $gq \rightarrow \gamma q$ , the "Compton scattering" subprocess. The cross section here, as for high- $p_T$  lepton pairs, will give direct information about the gluon density. We look forward to more detailed measurements of prompt photons and leptons with high  $p_T$ , and to a renewed interest in the problem of  $\gamma/\pi$  ratios at all values of  $p_T$ .

#### ACKNOWLEDGMENTS

We thank B. Cox, M. Dechantsreiter, R. Field, C. Goebel, and L. Resvanis for discussions and information.

This research was supported in part by the University of Wisconsin Research Committee with funds granted by the Wisconsin Alumni Research Foundation, and in part by the Department of Energy under Contract No. EY-76-C-02-0881, C00-881-102.

<sup>1</sup>R. M. Baltrusaitis *et al.*, in Proceedings of the High Energy Physics Conference of the European Physical Society, Geneva, 1979 (unpublished); Phys. Lett. **88B**, 372 (1979); B. Cox, talk at the 1979 International Symposium on Lepton and Photon Interactions at High Ener-

gies, Fermilab (unpublished).

<sup>2</sup>M. Diakonou *et al.*, in Proceedings of the High Energy Physics Conference of the European Physical Society, Geneva, 1979 (unpublished); Phys. Lett. **87B**, 292 (1979).

- <sup>3</sup>F. Halzen and D. M. Scott, *Phys. Rev. Lett.* **40**, 1117 (1978); *Phys. Rev. D* **18**, 3378 (1978).
- <sup>4</sup>R. Ruckl, S. Brodsky, and J. Gunion, *Phys. Rev. D* **18**, 2469 (1978).
- <sup>5</sup>A. P. Contogouris, S. Papadopoulos, and M. Hongoh, *Phys. Rev. D* **19**, 2607 (1979).
- <sup>6</sup>R. Field, in *Proceedings of the 19th International Conference on High Energy Physics, Tokyo, 1978*, edited by S. Homma, M. Kawaguchi, and H. Miyazawa (Phys. Soc. of Japan, Tokyo, 1979); lectures at La Jolla Workshop, 1978, Caltech Report No. CALT-68-696 (unpublished).
- <sup>7</sup>D. Jones and R. Ruckl, *Phys. Rev. D* **20**, 232 (1979).
- <sup>8</sup>Previous related speculations include C. O. Escobar, *Nucl. Phys.* **B98**, 173 (1975); *Phys. Rev. D* **15**, 355 (1977); G. R. Farrar and S. C. Frautschi, *Phys. Rev. Lett.* **36**, 1017 (1976); E. L. Feinberg, *Nuovo Cimento* **34A**, 391 (1976); G. R. Farrar, *Phys. Lett.* **67B**, 337 (1977); F. Halzen, Rutherford Report No. RL-77-049/A (unpublished); H. Fritzsch and P. Minkowski, *Phys. Lett.* **69B**, 316 (1977).
- <sup>9</sup>A. Donaldson *et al.*, *Phys. Rev. Lett.* **36**, 1110 (1976).
- <sup>10</sup>R. M. Baltrusaitis *et al.*, Fermilab report, 1979 (unpublished).
- <sup>11</sup>A. G. Clark *et al.*, *Phys. Lett.* **74B**, 267 (1978).
- <sup>12</sup>A. L. S. Angelis *et al.*, *Phys. Lett.* **79B**, 505 (1979).
- <sup>13</sup>F. W. Busser *et al.*, *Nucl. Phys.* **B106**, 1 (1976).
- <sup>14</sup>C. Kourkouvelis *et al.*, *Phys. Lett.* **83B**, 257 (1979).
- <sup>15</sup>D. Antreasyan *et al.*, *Phys. Rev. D* **19**, 764 (1979).
- <sup>16</sup>F. Halzen, in *Proceedings of the 19th International Conference on High Energy Physics, Tokyo, 1978* (Ref. 6); D. M. Scott, in *Lepton Pair Production in Hadron-Hadron Collisions*, proceedings of the Workshop, Bielefeld, 1978, edited by J. Cleymans (Univ. Bielefeld, Bielefeld, Germany, 1978).
- <sup>17</sup>G. Altarelli, G. Parisi, and R. Petronzio, *Phys. Lett.* **76B**, 356 (1978); see also F. Halzen and D. M. Scott, *Phys. Rev. D* **19**, 216 (1979).
- <sup>18</sup>L. M. Lederman, in *Proceedings of the 19th International Conference on High Energy Physics, Tokyo, 1978* (Ref. 6).
- <sup>19</sup>J. F. Owens and E. Reya, *Phys. Rev. D* **17**, 3003 (1978).
- <sup>20</sup>C. Kourkouvelis *et al.*, *Phys. Lett. B* (to be published).
- <sup>21</sup>C. Kourkouvelis *et al.*, *Phys. Lett.* **84B**, 271 (1979).
- <sup>22</sup>R. Blankenbecler, S. J. Brodsky, and J. F. Gunion, *Phys. Rev. D* **18**, 900 (1978).
- <sup>23</sup>F. Halzen and D. M. Scott, *Phys. Lett.* **79B**, 123 (1978).
- <sup>24</sup>See L. M. Lederman, *Phys. Rep.* **26**, 149 (1976); J. Cronin, in *Proceedings of the International Symposium on Lepton and Photon Interactions at High Energies, Hamburg, 1977*, edited by F. Gutbrod (DESY, Hamburg, 1977).
- <sup>25</sup>R. Ruckl, *Phys. Lett.* **64B**, 39 (1976).
- <sup>26</sup>Z. Kunszt and A. De Rújula (private communication from E. Reya).
- <sup>27</sup>S. Pakvasa, M. Dechantsreiter, F. Halzen, and D. M. Scott, *Phys. Rev. D* **20**, 2862 (1979).
- <sup>28</sup>E. L. Feinberg, *Izv. Akad. Nauk SSSR, Ser. Fiz.* **26**, 622 (1962); *Nuovo Cimento* **34A**, 391 (1976).
- <sup>29</sup>S. I. Nikolsky, International Cosmic Ray Conference, Leeds, 1976 (unpublished); Moscow Report No. 140, 1976 (unpublished).